An Anti-windup Fault Tolerant Control Scheme with Guaranteed Transient Performance for Tailless Flying Wing Aircraft

Shuang, Weifang; Zhang, Shaojie; Wu, Xue; van Kampen, Erik-Jan; Chu, Qiping

DOI
10.2514/6.2017-1253

Publication date
2017

Document Version
Accepted author manuscript

Published in
AIAA Guidance, Navigation, and Control Conference, 2017

This is an Accepted Manuscript of an article published in: AIAA Guidance, Navigation, and Control Conference
January 9-13, Grapevine, TX. ISBN: 978-1-62410-450-3
Available online: https://arc.aiaa.org/doi/10.2514/6.2017-1253

An Anti-windup Fault Tolerant Control Scheme with Guaranteed Transient Performance for Tailless Flying Wing Aircraft

Weifang Shuang, Shaojie Zhang, Xue Wu
Nanjing University of Aeronautics and Astronautics, Nanjing, Jiangsu, 211106, China

Erik-Jan van Kampen, Qiping Chu
Delft University of Technology, Delft, 2629 HS, The Netherlands

In this paper, the design of a constrained adaptive backstepping flight control law based on prescribed performance bound is discussed for a flying wing aircraft longitudinal control with actuator stuckness or failures, saturation nonlinearity of actuators considered. By prescribed performance, the convergence rate and maximum overshoot of the tracking errors are restrained within prespecified values. Faults of actuators are handled by online update laws which can estimate the fault parameters, thus reducing the effect of faults on control accuracy. Second-order low-pass command filters are introduced to limit the deflection angles of elevators and throttle levels, therefore avoiding saturation of actuators and the complex derivative computation in the backstepping process. In addition, control allocation strategy is designed to reduce the effect of faults on the lateral motion. The stability of the closed-loop system and the convergence of parameters are proved. Computer simulation shows that the closed-loop system is stable, the control law tracks reference trajectories well, and the actuators are within their physical limits in the presence of actuator faults.

I. Introduction

Tailless flying wing aircraft [1-3] have gotten wide research and application in fighters for their light weight, good stealth and flexible maneuverability, and have been deemed to be a new trend of civil aircraft. However, it is the flying wing layout that brings about some new challenges for flying wing aircraft [4-5]. Without a horizontal tail, flying wing aircraft have bad longitudinal stability and maneuverability for short moment arm. Without a vertical tail, they have bad lateral stability. Advanced control surfaces are introduced, including elevons that can achieve both pitching and rolling control and drag rudders that work as both rudders and drag plates, which results in serious coupling between the control surfaces. Therefore, there exist many problems difficult to solve with the traditional control methods, and it's very necessary to study new methods for the flying wing aircraft control systems. Moreover, actuators are the components of systems most prone to failures due to the frequent execution of tasks. And physical limitations impose magnitude, rate, and bandwidth constraints on the control surface deflections and the aircraft states. Problems researchers face are how to design fault-tolerant control (FTC) laws of tailless flying wing aircraft with actuator failures, how to reasonably allocate the desired control to each surfaces for maximum control efficiency, and how to avoid saturation of control surfaces.

However, the existing literatures on FTC of tailless flying wing aircraft with actuator failures are rare. Direct adaptive compensation control [6-9], a kind of active FTC[10-11], has been widely studied and applied, because it needs neither fault diagnosis and isolation unit nor readjustment of the form of control law in the presence of failures. In [12], a backstepping adaptive compensation control law is designed for a class of multi input and multi output (MIMO) systems with combined actuator faults, with the outputs of the system tracking the reference signals stably and asymptotically. But the saturation of control surfaces is not under consideration, and the method can only be applied to systems that can be transformed into lower triangular form. In [13] and [14], command filters are introduced to implement the constraints on the control surfaces and the virtual control states by J. A. Farrell et al. In [13], a command filtered backstepping control method, which covers all affine nonlinear systems, except for systems with uncertain parameters, is proposed for a known system with input constraints. In [14], a command filtered adaptive backstepping control method is proposed, with uncertain system parameters estimated by adaptive parameter adjustment law. Thus it is applicable to systems with control surface failures. But the author designs the control law aiming at single input single output (SISO) systems and using first order command filters. In [15], a command filtered adaptive backstepping control law is designed to solve the FTC problem of conventional aircraft with structural damage, and a good result is achieved. However, the command filters are aiming at avoiding the tedious analytic computation of virtual control signal derivatives and the constraints on the control surfaces and the virtual control states aren't implemented. Hence, the control efficiency will be discounted in the presence of saturation. Additionally, because of the uncertainty of the actuator faults, the system can't get guaranteed transient performance. In [16], authors propose the prescribed performance bound (PPB) based design way, which can characterize the convergence rate and the maximum overshoot of the tracking error, to improve the transient performance of adaptive systems. The tracking errors can be guaranteed within the prescribed error bounds all the time as long as the stability of the transformed error system is ensured. The scheme of [16] is further extended to MIMO nonlinear systems in [17-18].

In this article, for a MIMO flying wing aircraft system with stuck or partial loss failures of the actuators, we analyze the characteristics of failures and propose a command filtered adaptive backstepping approach based on PPB. Prescribed error bounds are given to improve the transient performance of the system. Online estimation of fault parameters compensates the effect of actuator failures on control accuracy. Second order command filters are employed to accommodate magnitude, rate, and bandwidth constraints on the actuator signals as well as the intermediate control variables used in the backstepping control approach. The effects of these constraints on the inputs and states are estimated by first-order filters and removed from the parameter update laws so that the parameter estimation process will be stable even when these limitations are in effect. In addition, control allocation strategy can reduce the effect of faults on the lateral motion. An additional advantage of this approach is that the two other main drawbacks of the adaptive backstepping methods are also eliminated, that is, the tedious analytic computation of virtual control signal derivatives and the restriction to nonlinear systems of lower triangular form. At last, the stability of the closed-loop system and the convergence of parameters are proved. Computer simulation shows that the control law has good tracking even when actuators fail.

II. Aircraft Dynamics

The control law design is based on the nonlinear longitudinal model of a tailless flying wing aircraft which has an aerodynamic layout with an s-shaped inlet arranged on the surface of blended wing body, two inboard engines by the two sides of the body, and three single undercarriages set in a triangle. All the control surfaces are set by the serrated trailing edge in the shape of "double W", including three pairs of elevons, a pair of drag rudders and a "beaver tail". Among them, two pairs of elevons are used as elevators and ailerons respectively, another one as redundant control surfaces, drag rudders as rudders as well as speed brake, "beaver tail" as the surface for longitudinal trim. All the control surfaces are in their mechanical limitations, elevons in $-25° \sim +25°$, and drag rudders in $0° \sim \pm 90°$. The control surfaces are arranged as Fig. 1.

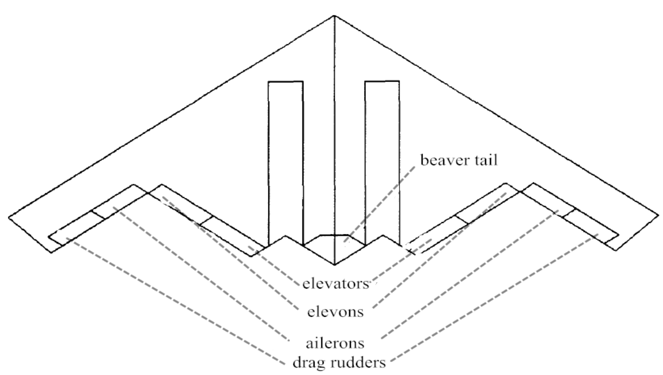

Figure 1. Configuration diagram of control surfaces

First, make the following assumptions about the aircraft and its flight environment: the earth is the inertial reference frame; the plane is a rigid body and its mass is a constant; the acceleration of gravity does not vary with altitude; the density of the atmosphere is a constant. In addition, assume that three pairs of elevons have equivalent control efficiency, that is, the same deflection angles of them cause the same pitching or rolling moments. Referring the aircraft-body coordinate frame, a kinematics equation of six freedom degree describing the motion of the aircraft is established, specific parameters in [19]. The longitudinal model, obtained by decoupling with two control inputs, including two engine throttle and two pairs of elevators (elevons in Fig. 1, hereinafter called as elevators collectively), can be expressed as

$$\begin{aligned} \dot{V} &= f_1 + G_1 u_t \\ \dot{\alpha} &= f_2 + G_2 u_t \\ \dot{\theta} &= q \\ \dot{q} &= f_4 + G_4 u_e \end{aligned} \tag{1}$$

where V is the velocity, α is the attack angle, θ is the pitch angle, q is the pitch rate. The input u_t is the total engine throttle level, i.e., $u_t = (u_{t1} + u_{t2})$. The input u_e is the total elevator angle, i.e., $u_e = (u_{e1} + u_{e2} + u_{e3} + u_{e4})$, where u_{e1} and u_{e2} are the deflection angles of left and right inner elevators, u_{e3} and u_{e4} are the angles of left and right outer elevators. f_1, f_2, f_4, G_1, G_2, G_4 are as follows.

$$\begin{aligned} f_1 &= -\frac{1}{2m}\rho V^2 S[C_{D0} + k(C_{L\alpha}\alpha + \frac{c_A}{2V}C_{Lq}q + \frac{c_A}{2V}C_{L\dot{\alpha}}\dot{\alpha})^2] - g_1 \\ f_2 &= q - \frac{1}{2m}\rho V S(C_{L\alpha}\alpha + \frac{c_A}{2V}C_{Lq}q + \frac{c_A}{2V}C_{L\dot{\alpha}}\dot{\alpha}) + \frac{1}{V}g_2 \\ f_4 &= \frac{1}{2I_y}\rho V^2 S c_A(C_{m0} + C_{m\alpha}\alpha + \frac{c_A}{2V}\cdot C_{mq}q + \frac{c_A}{2V}C_{m\dot{\alpha}}\dot{\alpha}) + \frac{1}{I_y}z_T T_{\max} u_t \end{aligned} \tag{2}$$

$$G_1 = \frac{1}{m}T_{\max}\cos\alpha,\ G_2 = -\frac{1}{mV}T_{\max}\sin\alpha,\ G_4 = \frac{1}{2I_y}\rho V^2 S c_A C_{mu_e} \tag{3}$$

where m is the mass, S is the wing area, ρ is the air density, c_A is the mean aerodynamic chord, I_y is the moment of inertia. $T_{\max}$ is the maximum thrust of one engine and C_{mu_e} is the pitching moment coefficient of one piece of elevator. $C_{L\alpha}$, C_{Lq}, $C_{L\dot{\alpha}}$ and C_{D0} are the aerodynamic derivatives about lift or drag. $g_1 = g(\cos\alpha\sin\theta - \sin\alpha\cos\theta)$, $g_2 = g(\sin\alpha\sin\theta + \cos\alpha\cos\theta)$, and g is the acceleration of gravity.

The *i*th actuator failure to be considered is modeled as

$$u_{ei} = \lambda_i u_{eci}(t) + \bar{u}_{ei},\ Rank(diag\{\lambda_i, \bar{u}_{ei}\}) \le 1,\ t \ge t_i, 0 \le \lambda_i \le 1, i = 1, \cdots, 4 \tag{4}$$

where u_{eci} is the fault free actuator output and u_{ei} is the faulty actuator output of the *i*th elevator, $\lambda_i \in R$ is the actuator effectiveness, and $\bar{u}_{ei} \in R$ is the stuck position. Equation (4) can represent the following four failure cases, in which no-failure, stuck-in-space failure, loss of effectiveness and float type of failure are included.

① $\lambda_i = 1$ and $\bar{u}_i = 0$

In this case, the *i*th actuator is regarded as a failure-free actuator.

② $0 < \lambda_i < 1$ and $\bar{u}_i = 0$

This case indicates partial loss of effectiveness of the *i*th actuator. For example, $\lambda_i = 0.6$ means that the *i*th actuator loses 40% of its effectiveness.

③ $\bar{u}_i \ne 0$ and $\lambda_i = 0$

This case indicates that the *i*th actuator is stuck at $\bar{u}_i$.

④ $\lambda_i = 0$ and $\bar{u}_i = 0$

This case indicates that the *i*th actuator has lost its effectiveness totally.

The control objective is to design a fault-tolerant control law for plant (1) with failures (4) so that the closed-loop system can keep stable and track the given reference signals asymptotically.

III. Nonlinear Fault-tolerant Controller Design

The The reference signals are

$$V = V_r,\ \theta = \theta_r \tag{5}$$

First, two assumptions are given.

Assumption 1 The state variable $[\alpha,\theta]$ belongs to a compact set $\Omega_c = \{[\alpha,\theta] \| |\alpha| \le 30^\circ, |\theta| \le 45^\circ\}$.

Assumption 2 The desired tracking trajectories satisfy that V_r, $\dot{V}_r$, $\ddot{V}_r$, θ_r, $\dot{\theta}_r$, $\ddot{\theta}_r$ are all bounded.

Only assumption 1 stands, can the aerodynamic coefficients in (2) be viewed as constants, thus does system (1) make sense. If the reference trajectories are continuous and smooth, assumption 2 will hold.

Then, the definition of command filter is given as follows. We choose a second-order low-pass command filter and express it with $[q_1, q_2]^T$. Assume that the signal to be treated is α_c^0, then the command filter is defined as (6).

$$\begin{bmatrix} \dot{q}_1(t) \\ \dot{q}_2(t) \end{bmatrix} = \begin{bmatrix} q_2 \\ 2\zeta\omega_n \left[S_R\left(\frac{\omega_n}{2\zeta}\left[S_M(\alpha_c^0, M_L, M_U) - q_1 \right], R_L, R_U \right) - q_2 \right] \end{bmatrix}$$
$$\begin{bmatrix} \alpha_c \\ \dot{\alpha}_c \end{bmatrix} = \begin{bmatrix} q_1 \\ q_2 \end{bmatrix} \tag{6}$$

where $S_M(*, M_L, M_U)$ and $S_R(*, R_L, R_U)$ represent the magnitude and rate limit functions, respectively. These saturation functions are defined similarly as

$$S_M(*, M_L, M_U) = \begin{cases} M_L & \text{if } x \le M_L \\ x & \text{if } M_L \le x \le M_U \\ M_U & \text{if } x \ge M_U \end{cases} \tag{7}$$

The desired virtual control signal α_c^0 is filtered to produce the magnitude, rate, and bandwidth limited virtual control signal α_c and its derivative $\dot{\alpha}_c$ that satisfy the limits imposed on the control variable.

A. Prescribed Performance Bound Based Transformed System

The objective in this section is to ensure the transient performance in the sense that the tracking errors $e_1 = V - V_r$, $e_2 = \theta - \theta_r$ are preserved within a specified PPB all the time no matter when actuator failures occur. The tracking errors are desired to satisfy the conditions that

$$-\underline{\delta}_i \tau_i(t) < e_i(t) < \bar{\delta}_i \tau_i(t), \forall t \ge 0, \quad i = 1, 2 \tag{8}$$

where $0 < \underline{\delta}_i, \bar{\delta}_i \le 1$, $\tau_i(t)$ are the performance functions to be designed as smooth and decreasing functions with $\tau_{i0} > \lim_{t\to\infty} \tau_i(t) = \tau_{i\infty} > 0$. Then, if $e_i(t)$ can meet condition (8) under the designed control law, the tracking errors will be bounded and $-\underline{\delta}_i \tau_{i\infty} < \lim_{t\to\infty} e_i(t) = \bar{\delta}_i \tau_{i\infty}$.

First, a strictly increasing function $S(v)$ is designed to meet the following conditions

$$-\underline{\delta} < S(v) < \bar{\delta}; \ \lim_{v\to+\infty} S(v) = \bar{\delta}, \lim_{v\to-\infty} S(v) = -\underline{\delta}; \ S(0) = 0 \tag{9}$$

Then, if $e_i(t) = \tau_i(t) S(v_i)$, $e_i(t)$ can meet condition (8). Hence, we design $S(v)$ as

$$S(v) = \frac{\bar{\delta} e^{(v+r)} - \underline{\delta} e^{-(v+r)}}{e^{(v+r)} + e^{-(v+r)}} \tag{10}$$

where $r = (\ln(\underline{\delta}/\bar{\delta}))/2$. It can be proved that $S(v)$ meet condition (9). From (9) and (10), the transformed tracking errors v_i are solved as

$$v_i = \frac{1}{2}\ln(\bar{\delta}_i \varepsilon_i(t) + \bar{\delta}_i \underline{\delta}_i) - \frac{1}{2}\ln(\bar{\delta}_i \underline{\delta}_i - \underline{\delta}_i \varepsilon_i(t)) \tag{11}$$

where $\varepsilon_i(t) = e_i(t)/\tau_i(t)$. Differentiating (11), it follows that

$$\dot{v}_1 = \frac{\partial S^{-1}}{\partial \varepsilon_1}\dot{\varepsilon}_1 = \zeta_1(\dot{V} - \dot{V}_r - \frac{e_1\dot{\tau}_1}{\tau_1})$$
$$\dot{v}_2 = \frac{\partial S^{-1}}{\partial \varepsilon_2}\dot{\varepsilon}_2 = \zeta_2(\dot{\theta} - \dot{\theta}_r - \frac{e_2\dot{\tau}_2}{\tau_2}) \tag{12}$$

where $\zeta_i = \frac{1}{2\tau_i}[\frac{1}{\varepsilon_i + \underline{\delta}_i} - \frac{1}{\varepsilon_i - \bar{\delta}_i}]$. Then, system (1) can be transformed based on PPB to

$$
\begin{aligned}
\dot{v}_1 &= \zeta_1 (f_1 + G_1 u_t - \dot{V}_r - \frac{e_1 \dot{\tau}}{\tau}) \\
\dot{v}_2 &= \zeta_2 (q - \dot{\theta}_r - \frac{e_2 \dot{\tau}}{\tau}) \\
\dot{q} &= f_4 + G_4 u_e
\end{aligned} \tag{13}
$$

From the above transformation, if $\lim_{t\to\infty} v_i(t) = 0$ holds under the designed control law, $e_i(t)$ will be bounded and approach to zero.

B. Design of the control law

The command filtered adaptive backstepping control law can be designed according to Fig. 2. The nominal virtual control law to be designed is denoted as $[u_{tc}^0, q_c^0, u_{ec}^0]^T$, and the available virtual control law is denoted as $[u_{tc}, q_c, u_{ec}]^T$. The tracking errors of system (13) are defined as

$$
\begin{aligned}
z_{11} &= v_1 \\
z_{21} &= v_2 \\
z_{22} &= q - \dot{\theta}_r - q_c
\end{aligned} \tag{14}
$$

If saturation does occur, the actual tracking errors z_{ij} may increase. Thus, it's necessary to introduce the tracking complementary signals χ_{ij} to indicate the effect of the state constraints on the tracking errors $e_i(t)$ · χ_{ij} are expressed as

$$
\begin{bmatrix} \dot{\chi}_{11} \\ \dot{\chi}_{21} \\ \dot{\chi}_{22} \end{bmatrix} = - \begin{bmatrix} c_{11}\chi_{11} \\ c_{21}\chi_{21} \\ c_{22}\chi_{22} \end{bmatrix} + \begin{bmatrix} G_1 (u_{tc} - u_{tc}^0) \\ (q_c - q_c^0) \\ G_4 (u_{ec} - u_{ec}^0) \end{bmatrix} \tag{15}
$$

where $c_{11}, c_{21}, c_{22} > 0$ are the controller gains to be designated, and the initial values of χ_{ij} are zeros, that is, $[\chi_{11}; \chi_{21}; \chi_{22}](0) = \mathbf{0}$. From (12), the effect of input and state constraints on the tracking errors v_i can be defined as $\varsigma_i \chi_{i1}$. Thus, the modified tracking errors are

$$
\begin{bmatrix} \bar{z}_{11} \\ \bar{z}_{21} \\ \bar{z}_{22} \end{bmatrix} = \begin{bmatrix} z_{11} - \varsigma_1 \chi_{11} \\ z_{21} - \varsigma_2 \chi_{21} \\ z_{22} - \chi_{22} \end{bmatrix} \tag{16}
$$

To guarantee the stability of the closed-loop system, we design the nominal virtual control laws as

$$
\begin{aligned}
u_{tc}^0 &= \frac{1}{G_1} (-\frac{c_{11} z_{11}}{\varsigma_1} + \dot{V}_r - f_1 + \frac{e_1 \dot{\tau}}{\tau}) \\
q_c^0 &= -\frac{c_{21} z_{21}}{\varsigma_2} + \bar{z}_{22} + \dot{\theta}_r + \frac{e_2 \dot{\tau}}{\tau} \\
u_{ec}^0 &= \frac{1}{G_4} (-c_{22} z_{22} - \varsigma_2 \bar{z}_{21} - f_4 + \dot{q}_c + \ddot{\theta}_r)
\end{aligned} \tag{17}
$$

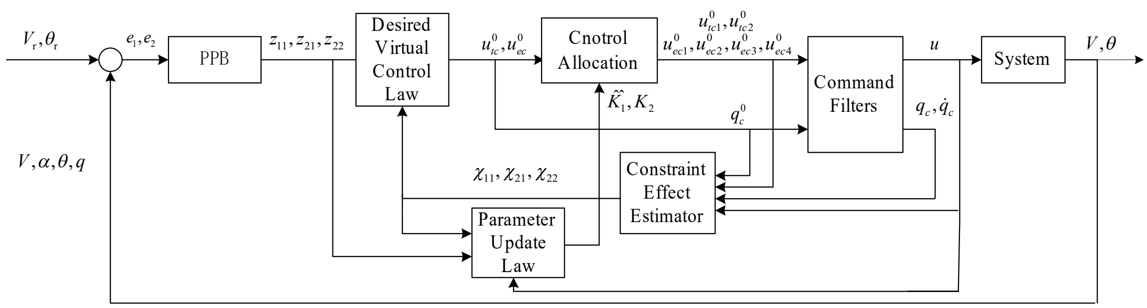

Figure 2. Control scheme of the system

For the flying wing aircraft, control surfaces have high redundancy. The virtual control law shall be allocated to each of the surfaces. Denote the final control law to be designed as $u=[u_{tc1},u_{tc2},u_{ec1},u_{ec2},u_{ec3},u_{ec4}]^T$, and the corresponding desired control law is $[u_{tc1}^0,u_{tc2}^0,u_{ec1}^0,u_{ec2}^0,u_{ec3}^0,u_{ec4}^0]^T$. Assume that the elevators fall into failures (4), and denote $K_1=diag\{\lambda_1,\lambda_2,\lambda_3,\lambda_4\}$, $K_{1i}=\lambda_i,\ i=1,2,3,4$; $K_2=\bar{u}_e=[\bar{u}_{e1},\bar{u}_{e2},\bar{u}_{e3},\bar{u}_{e4}]^T$. In order to decrease the possibility of the aircraft's going into rolling or yawing, design the desired control laws of each input as

$$
\begin{aligned}
&u_{tc1}^0=u_{tc2}^0=\frac{1}{2}u_{tc}^0\\
&u_{eci}^0=\begin{cases}\dfrac{1}{2\hat{K}_{1i}}[\dfrac{1}{2}u_{ec}^0-(N_1+N_3)^T\hat{K}_2],\ i=1,3\\ \dfrac{1}{2\hat{K}_{1i}}[\dfrac{1}{2}u_{ec}^0-(N_2+N_4)^T\hat{K}_2],\ i=2,4\end{cases}
\end{aligned}
\tag{18}
$$

where, $N_i\in R^{4\times1}(i=1,2,3,4)$ is a column vector of which the *i*th element is 1 and the other elements are 0. $\hat{K}_{1i}$ and $\hat{K}_2$ are the estimates of K_{1i} and K_2 respectively. The parameter update laws are designed as

$$
\begin{aligned}
&\dot{\hat{K}}_{1i}=\frac{1}{\Gamma_{1i}}\bar{z}_{22}G_4u_{eci},\ i=1,2,3,4\\
&\dot{\hat{K}}_2=\Gamma_2^{-1}\bar{z}_{22}G_4(N_1+N_2+N_3+N_4)
\end{aligned}
\tag{19}
$$

where $\Gamma_1=diag\{\Gamma_{11},\Gamma_{12},\Gamma_{13},\Gamma_{14},\}\in R^{4\times4}>0$, $\Gamma_2\in R^{4\times4}>0$ are positive definite adaptation gain matrices. The desired virtual control signal q_c^0 is filtered to generate the magnitude, rate, and bandwidth limited virtual control signal q_c and its derivative $\dot{q}_c$. The desired control signal $[u_{tc1}^0,u_{tc2}^0,u_{ec1}^0,u_{ec2}^0,u_{ec3}^0,u_{ec4}^0]^T$ is filtered to generate the magnitude, rate, and bandwidth limited control signal $[u_{tc1},u_{tc2},u_{ec1},u_{ec2},u_{ec3},u_{ec4}]^T$ and its derivative $[\dot{u}_{tc1},\dot{u}_{tc2},\dot{u}_{ec1},\dot{u}_{ec2},\dot{u}_{ec3},\dot{u}_{ec4}]^T$. Thus, the virtual control signals u_{tc} and u_{ec} have

$$
\begin{aligned}
&u_{tc}=u_{tc1}+u_{tc2}\\
&u_{ec}=\sum_{i=1}^{4}\lambda_iu_{eci}+\bar{u}_i=(N_1+N_2+N_3+N_4)^T\bullet(\hat{K}_1[u_{ec1},u_{ec2},u_{ec3},u_{ec4}]^T+K_2)
\end{aligned}
\tag{20}
$$

IV. Stability Analysis

Theorem 1 For system (1), control law (17) and parameter update law (19) can ensure that all the variables are bounded and the modified tracking errors $\bar{z}_{ij}$ approach to zero asymptotically.

Proof Under the former definitions, differentiate (16), and substitute (14), (15), (17), and (20), then we can get

$$
\begin{aligned}
\dot{\bar{z}}_{11} &= \dot{z}_{11} - \varsigma_1\dot{\chi}_{11} = \varsigma_1(f_1 + G_1 u_{tc} - \dot{V}_r - \frac{e_1\dot{\tau}}{\tau}) + c_{11}\varsigma_1\chi_{11} - \varsigma_1 G_1(u_{tc} - u_{tc}^0) \\
&= \varsigma_1(f_1 - \dot{V}_r + c_{11}\chi_{11}) - c_{11}z_{11} + \varsigma_1(\dot{V}_r - f_1) = -c_{11}\bar{z}_{11} \\
\dot{\bar{z}}_{21} &= \dot{z}_{21} - \varsigma_2\dot{\chi}_{21} = \varsigma_2(q - \dot{\theta}_r - \frac{e_2\dot{\tau}}{\tau}) + c_{21}\varsigma_2\chi_{21} - \varsigma_2(q_c - q_c^0) \\
&= c_{21}\varsigma_2\chi_{21} - c_{21}z_{21} + \varsigma_2\bar{z}_{22} = -c_{21}\bar{z}_{21} + \varsigma_2\bar{z}_{22} \\
\dot{\bar{z}}_{22} &= \dot{z}_{22} - \dot{\chi}_{22} = \dot{q} - \ddot{\theta}_r - \dot{q}_c + c_{22}\chi_{22} - G_4(u_{ec} - u_{ec}^0) \\
&= f_4 + G_4 u_e - \ddot{\theta}_r - \dot{q}_c + c_{22}\chi_{22} - G_4 u_{ec} - c_{22}z_{22} - \varsigma_2\bar{z}_{21} - f_4 + \dot{q}_c + \ddot{\theta}_r \\
&= -c_{22}\bar{z}_{22} - \varsigma_2\bar{z}_{21} + G_4(\sum_{i=1}^{4} K_{1i}u_{eci} + \sum_{i=1}^{4} K_{2i} - \sum_{i=1}^{4}\hat{K}_{1i}u_{eci} - \sum_{i=1}^{4} K_{2i}) \\
&= -c_{22}\bar{z}_{22} - \varsigma_2\bar{z}_{21} - G_4[\sum_{i=1}^{4}\tilde{K}_{1i}u_{eci} + (N_1 + N_2 + N_3 + N_4)^T\tilde{K}_2]
\end{aligned}
\tag{21}
$$

where $\tilde{K}_{1i} = \hat{K}_{1i} - K_{1i}$, $\tilde{K}_2 = \hat{K}_2 - K_2$. Define a positive definite $V_L(t)$ as

$$
V_L(t) = \frac{1}{2}\bar{z}_{11}^2 + \frac{1}{2}\bar{z}_{21}^2 + \frac{1}{2}\bar{z}_{22}^2 + \frac{1}{2}tr[\tilde{K}_1^T\Gamma_1\tilde{K}_1] + \frac{1}{2}\tilde{K}_2^T\Gamma_2\tilde{K}_2
\tag{22}
$$

Differentiating $V_L(t)$, we get

$$
\begin{aligned}
\dot{V}_L(t) &= -c_{11}\bar{z}_{11}^2 - c_{21}\bar{z}_{21}^2 - c_{22}\bar{z}_{22}^2 - \bar{z}_{22}G_4\cdot[\sum_{i=1}^{4}\tilde{K}_{1i}u_{eci} + (N_1 + N_2 + N_3 + N_4)^T\tilde{K}_2] + tr[\tilde{K}_1^T\Gamma_1\dot{\tilde{K}}_1] + \dot{\tilde{K}}_2^T\Gamma_2^{-1}\tilde{K}_2 \\
&= -c_{11}\bar{z}_{11}^2 - c_{21}\bar{z}_{21}^2 - c_{22}\bar{z}_{22}^2 + \sum_{i=1}^{m}[\tilde{K}_{1i}(-\bar{z}_{22}G_4 u_{eci} + \Gamma_{1i}\dot{\tilde{K}}_{1i})] + (\dot{\tilde{K}}_2^T\Gamma_2 - \bar{z}_{22}G_4(N_1 + N_2 + N_3 + N_4)^T)\tilde{K}_2
\end{aligned}
\tag{23}
$$

Substituting (19) into (23), with $\dot{\tilde{K}}_1 = \dot{\hat{K}}_1, \dot{\tilde{K}}_2 = \dot{K}_2$, we get

$$
\dot{V}_L(t) = -c_{11}\bar{z}_{11}^2 - c_{21}\bar{z}_{21}^2 - c_{22}\bar{z}_{22}^2 \le 0
\tag{24}
$$

$\dot{V}_L(t)$ is negative definite, which means that the closed-loop system is stable. Under the assumption 2, $\bar{z}_{11}$, $\bar{z}_{21}$, $\bar{z}_{22}$, $\tilde{K}_1$, and $\tilde{K}_2$ are bounded, thus $V_L(t)$ is bounded. Hence,

$$
\int_0^\infty(\bar{z}_{11}^2 + \bar{z}_{21}^2 + \bar{z}_{22}^2)\mathrm{d}t \le -\frac{1}{c}\int_0^\infty \dot{V}_L(t)\mathrm{d}t = -\frac{1}{c}(V_L(\infty) - V_L(0)) < \infty
\tag{25}
$$

where $c = \min\{c_{11}, c_{21}, c_{22}\}$. $\dot{\bar{z}}_{11}$, $\dot{\bar{z}}_{21}$, and $\dot{\bar{z}}_{22}$ exist and are bounded according to (21). Using the Barbalat theorem [20], it follows that

$$
\lim_{t\to\infty}\bar{z}_{11} = 0,\ \lim_{t\to\infty}\bar{z}_{21} = 0,\ \lim_{t\to\infty}\bar{z}_{22} = 0
\tag{26}
$$

Hence, the closed-loop system is asymptotically stable and the modified tracking errors approach to zero asymptotically. This means that during periods when there is no saturation, $\bar{z}_{ij}$ will converge to z_{ij}. If saturation does occur, the actual tracking errors z_{ij} may increase, but the modified tracking errors $\bar{z}_{ij}$ will still converge to zero and the estimation process remains stable. Thus, $e_i(t)$ are bounded and approach to zero. Under the control law (17) and parameter adjust law (19), system (1) is stable and tracks the given signals asymptotically.

V. Simulation Result

Under a cruising altitude of 11 kilometres and velocity of Ma 0.6, the flying wing aircraft is trimmed at 4 degree's angle of attack, 4 degree's pitching angle, 0.3041's throttling level and -7.1742 degree's deflection of elevators. View u_{t1} and u_{t2} as the variations of two throttling levels, then $u_t = u_{t1} + u_{t2} + 0.3041$. Assume that the beaver tail can offer the total pitching moment for trimming, then the trimming deflection of elevators can be treated as zero. That is, $u_e = (u_{e1} + u_{e2} + u_{e3} + u_{e4})$.

The reference velocity signal is $V_r = 130 + 20\cos(0.1t)$, and the reference pitching angle signal is $\theta_r = 18 + 10\sin(0.1t)$. The prescribed performance bounds are $\tau_1(t) = 48.7\mathrm{e}^{-0.2t} + 1.3$, $\underline{\delta}_1 = 0.5$, $\overline{\delta}_1 = 1$ and $\tau_2(t) = 7.7\mathrm{e}^{-0.2t} + 0.3$, $\underline{\delta}_2 = 0.8$, $\overline{\delta}_2 = 1$. The left inner elevator u_{e1} is stuck at -13 degree after 80 s, and the right inner elevator u_{e2} loses 60% of its effectiveness after 120 s.

Saturation limits of command filters in range and deflection rate are listed; see Table 1. Tune the controller gains, frequency and damp ratio of the command filters and parameter update law gains until the designated states track the reference signals best. Table 2 shows the selected command filter parameters. Figs. 3-7 show the simulation results.

Fig. 3 shows the designated states tracking the reference signals with the constraint of PPB or based on the normal method, where the red lines represent the reference trajectories and the blue lines the responses. It can be seen that the two control laws have no problem following the reference trajectories, except for a little tracking error of the velocity at the beginning because of the big difference between the trimmed velocity and the reference one. By the comparison of figs. 3 a) and b), it can be seen that the adaptive control law based on PPB has better tracking performance. To illustrate the superiority of PPB, figs. 4 shows the tracking errors, where the red lines represent the bounds and the blue lines the errors. In $t = 14 \sim 18s$, the tracking error of velocity in the normal case has exceeded the bound a little while that in PPB case is restrained within it. By the constraint of PPB, both the transient and

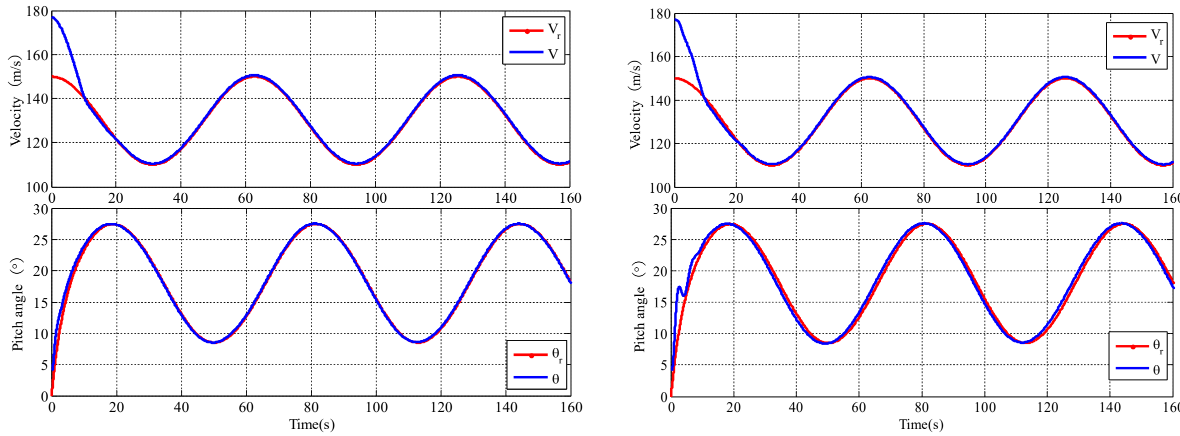

(a) PPB case **(b) Normal case**

Figure 3. Response curves of velocity and pitch angle

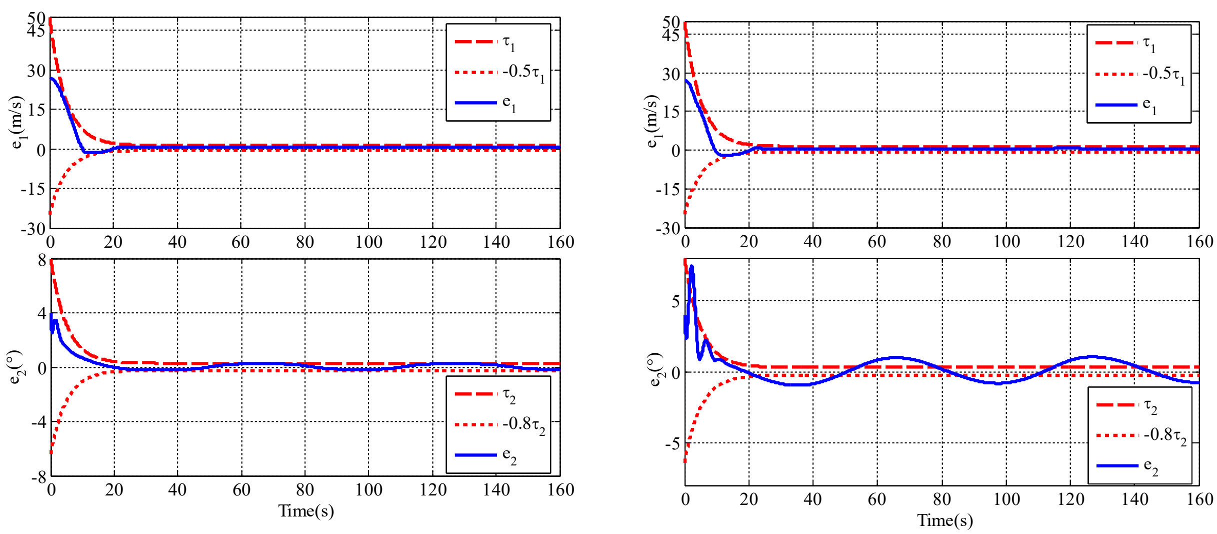

(a) PPB case **(b) Normal case**

Figure 4. Tracking errors of velocity and pitch angle

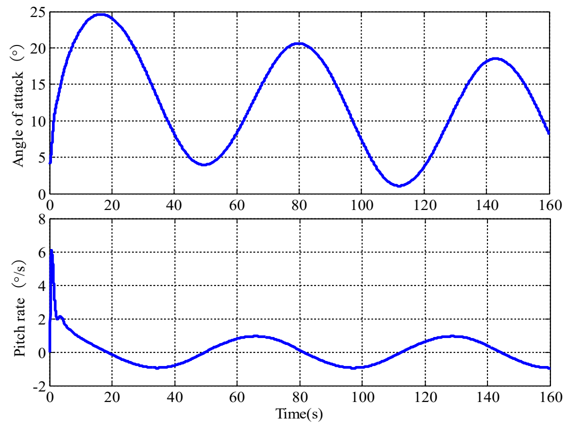

Figure 5. Response curves of angle of attack and pitch rate

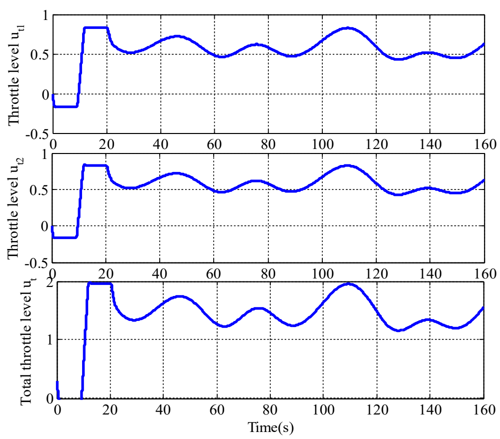

Figure 6. Varying curves of throttle levels

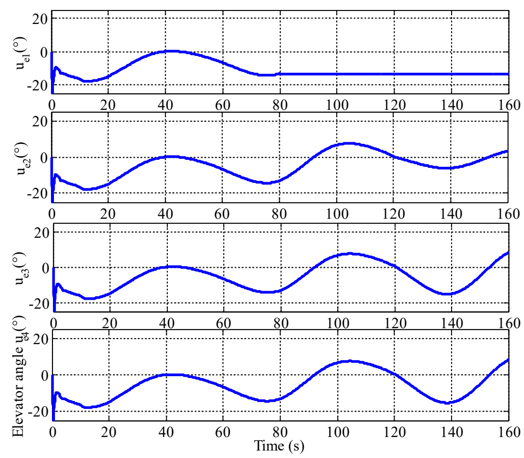

Figure 7. Varying curves of deflection angles of elevators

Command variable	Amplitude limit	Rate limit
u_{tc1}、u_{tc2}	$[0,1]$	$[0,0.4]\ \mathrm{s}^{-1}$
q_c	±35 deg/s	—
u_{ec1}、u_{ec2} u_{ec3} u_{ec4}	±25 deg	±60 deg/s

Table 1. Saturation limits

Parameters	Values
Control law gain c_{11}	1
Control law gain c_{21}	2
Control law gain c_{22}	25
Command filter frequency of u_t	5 rad/s
Command filter damp ratio of u_t	0.8
Command filter frequency of q	5 rad/s
Command filter damp ratio of q	0.8
Command filter frequency of u_e	35 rad/s
Command filter damp ratio of u_e	0.8
Adjustment law gain Γ_1	$\mathrm{diag}([200,200,200,200])$
Adjustment law gain Γ_2	$\mathrm{diag}([500,500,500,500])$

Table 2. Parameters of the controllers

steady performance of the tracking error of pitch rate are improved obviously from figs. 4. In addition, in PPB case, the steady-state error of velocity is about 0.5 and that of pitch rate is between -0.18 and 0.25, which are both within the desired bounds.

Fig. 5 shows the response curves of the angle of attack and the pitch rate. It can be seen that the system is basically stable without big up and down, except for an apparent oscillation at the beginning for velocity tracking. Fig. 6 shows the curves of throttle level variations of two engines and the total level, from which it can be seen that the two throttle levels come into saturation at some observational stages, but the control commands won't exceed the limits for the sake of command filters. Fig. 7 shows the curves of deflection of four elevators. At 80 s, u_{e1} is stuck, thus deflection of the other three elevators increase fast; u_{e2} loses partial effectiveness at 120 s, thus deflection of the other two elevators increase fast. That is, when some elevators fall into failures considered in this paper, the redundant control surfaces will work to compensate the bad influence of faults. Hence, the velocity, angle of attack, pitch angle and pitch rate have no obvious fluctuation. It's also apparent from Fig. 7 that deflection of all elevators comes into saturation at the beginning, but the control commands won't exceed the limits for the sake of command filters. Hence, under the control variables shown in Figs. 6-7 the tracking effectiveness in Fig. 3 is available for an actual aircraft. If command filters are not introduced to the control law, the desired control signals will exceed the mechanical limits of actuators and the tracking effectiveness will be discounted for actual aircraft.

VI. Conclusion

The proposed command filtered adaptive backstepping flight control law based on PPB has good fault tolerance ability and can avoid saturation of actuators, and the system could get guaranteed transient performance. Appropriate designated parameters can ensure that the closed-loop system keeps stable and tracks the given reference signals well. Simulation results verify the validity of the proposed method. For a flying wing aircraft, with actuator stuckness or loss of effectiveness, the control of lateral part is much more difficult, which will be studied next.

Acknowledgments

This work is supported by the National Nature Science Foundation of China under Grants 61473147.

References

[1]Song B. F., Zhang B. Q., Han Z. H., "The study of concept design criteria for large-scale passenger aircraft with new technologies," Acta Aeronautica et Astronautica Sinica , vol. 29, No. 3, 25 May 2008, pp. 583-595.

[2]Bowers A., NASA Dryden Flight Research Center, "Blended-Wing-Body: design challenges for the 21st century," Proceedings of The Wing Is The Thing (TWITT) meeting, 2000.

[3]Statzer M., Williams B., Zauberman M., "Flying wing," Mar. 2003.

[4]Meng X. R., Ma H. Z., "Summary for control method of flying wing UAV," Aerodynamic Missile Journal, vol. 5, 15 May 2015, pp. 25-28.

[5]Tomac M., Stenfelt G., "Predictions of stability and control for a flying wing," Aerospace Science and Technology, vol. 39, 2014, pp. 179-186.

[6]Tao G., "Direct adaptive actuator failure compensation control: a tutorial," Journal of Control & Decision, vol. 1, No. 1, 2014, pp. 75-101.

[7]Ma Y., Jiang B., Tao G., Cheng Y., "A direct adaptive actuator failure compensation scheme for satellite attitude control systems," Proceedings of the Institution of Mechanical Engineers, Part G: Journal of Aerospace Engineering, vol. 228, 2014, pp. 542-556.

[8]Zhang S. J., Qiu X. W., Liu C. S., Hu S. S., "Adaptive actuator failure compensation control based on MMST grouping for a class of MIMO nonlinear systems," Acta Automatica Sinica, No. 11, 15 Nov. 2014, pp. 2445-2455.

[9]Zhang S. J., Qiu X. W., B. Jiang, Liu C. S., "Adaptive actuator failure compensation control based on MMST grouping for a class of MIMO nonlinear systems with guaranteed transient performance," International Journal of Control, vol. 88, No. 3, 2014, pp. 593-601.

[10]Zhang Y. M., Jiang J., "Bibliographical review on reconfigurable fault-tolerant control systems," Annual Reviews in Control, vol. 32, No. 2, 2008, pp. 229-252.

[11]Jiang B., Yang H., "Survey of the active fault-tolerant control for flight control system," Systems engineering and electronics, vol. 29, 2007, pp. 2106-2110.

[12]Tang X. D., Tao G., Joshi S. M., "Adaptive actuator failure compensation for nonlinear MIMO systems with an aircraft control application," Automatica, vol. 43, 2007, pp. 1869-1883.

[13]Farrell J. A., Polycarpou M., Sharma M., Dong W., "Command filtered backstepping," IEEE Transactions on Automatic Control, vol. 54, 2009, pp. 1391-1395.

[14]Dong W. J., Farrell J. A., Polycarpou M., Sharma M., "Command filtered adaptive backstepping," IEEE Transactions on Control Systems Technology, vol. 20, 2012, pp. 566-580.

[15]Wang Q., Li Q., Chen N., Song J. Y., "A nonlinear fault tolerant flight control method against structural damage," Acta Aeronautica et Astronautica Sinica, vol. 2, 2016, pp. 637-647.

[16]Bechlioulis C. P., Rovithakis G. A., "A low-complexity global approximation-free control scheme with prescribed performance for unknown pure feedback systems," Automatica, vol. 50, No. 4, 2014, pp. 1217-1226.

[17]Qiu X. W., Zhang S. J., Liu C. S., "Adaptive Compensation Control Considering the Transient Performance of a Class of MIMO Nonlinear Systems with Actuator Failures," Information and Control, vol. 43, No. 1, 15 Feb. 2014, pp. 63-67.

[18]Zhang S. J., Qiu X. W., Liu C. S., "Neural Adaptive Compensation Control for a Class of MIMO Uncertain Nonlinear Systems with Actuator Failures," Circuits, Systems, and Signal Processing, vol. 33, No. 6, Jun. 2014, pp. 1971-1984.

[19]Li F. S., "Research on overall optimization design method for aggressive tailless flying wing UAV," M.S. Dissertation, Aeronauticas Dept., Northwestern Polytechnical Univ., Xi-an, China, 2007.

[20]Khalil H. K., Nonlinear Systems, 3rd ed., Prentice Hall, New Jersey, 2002.